DEWAR, M. J. S., ZOEBISCH, E. G., HEALY, E. F. & STEWART, J. J. P. (1986). *QCPE Bull.* **6**, 24–25.
KAI, Y., KNOCHEL, P., KWIATKOWSKI, S., DUNITZ, J. D., OTH, J. F. M., SEEBACH, D. & KALINOWSKI, H. O. (1982). *Helv. Chim. Acta*, **65**, 137–161.
KLYNE, W. & PRELOG, V. (1960). *Experientia*, **16**, 521–523.
LAM, Y. L., HUANG, H. H. & HAMBLEY, T. W. (1990). *J Chem. Soc. Perkin Trans.* 2, pp. 2039–2043.
LAM, Y. L., KOH, L. L. & HUANG, H. H. (1992). To be published.
LAM, Y. L., TAN, B. G. & HUANG, H. H. (1990). *J. Mol. Struct.* **221**, 115–126.
REUTOV, O. A., BELETSKAYA, I. P. & BUTIN, K. P. (1978). *CH-Acids*. New York: Pergamon Press.
Siemens Analytical X-ray Instruments Inc. (1989). *SHELXTL-Plus*. Release 4.0. Madison, Wisconsin, USA.
TAN, B. G., CHIA, L. H. L. & HUANG, H. H. (1986). *J. Chem. Soc. Perkin Trans.* 2, pp. 2025–2030.
TAN, B. G., CHIA, L. H. L., HUANG, H. H., KUOK, M. H. & TANG, S. H. (1984). *J. Chem. Soc. Perkin Trans.* 2, pp. 1407–1413.
TAN, B. G., LAM, Y. L., HUANG, H. H. & CHIA, L. H. L. (1990). *J. Chem. Soc. Perkin Trans.* 2, pp. 2031–2038.
WOLFE, S. (1972). *Acc. Chem. Res.* **5**, 102–111.

Acta Cryst. (1993). B**49**, 123–130

Molecular Structures of L-Leu-L-Tyr, Gly-D,L-Met.*p*-Toluenesulfonate and L-His-L-Leu

BY JEANETTE A. KRAUSE, PAUL W. BAURES AND DRAKE S. EGGLESTON

SmithKline Beecham Pharmaceuticals, Department of Physical and Structural Chemistry, L-950, Box 1539, King of Prussia, PA 19406, USA

(*Received* 2 *July* 1991; *accepted* 8 *June* 1992)

Abstract

L-Leu-L-Tyr, (I), $C_{15}H_{22}N_2O_4$, $M_r = 294.35$, crystallizes from MeOH/5% dimethyl sulfoxide in the orthorhombic space group $P2_12_12_1$. $a = 5.644$ (1), $b = 12.094$ (3), $c = 22.548$ (4) Å, $V = 1539.0$ (5) Å^3, $Z = 4$, $D_x = 1.270$ g cm^{-3}, Cu $K\alpha$, $\lambda = 1.54184$ Å, $\mu = 7.228$ cm^{-1}, $F(000) = 632$, $T = 173$ K, final R (on F) $= 0.033$ for 1347 observations with $I \geq 2\sigma(I)$. (I) crystallizes as a zwitterion with the N-terminus protonated and the C-terminus ionized. The peptide backbone adopts a distorted *trans* antiparallel β pleated-sheet conformation, with principal torsion angles $\psi_1 = 163.7$ (2), $\omega_1 = 158.7$ (2), $\varphi_2 = -110.9$ (3) and $\psi_2 = 141.4$ (2)°. The leucyl residue is in the $g^-(tg^-)$ conformation while the tyrosyl residue adopts the g^- conformation, with the phenol ring twisted from the low-energy perpendicular position. Gly-D,L-Met.*p*-toluenesulfonate, (II), $C_7H_{15}N_2O_3S^+.C_7H_7O_3S^-$, $M_r = 378.47$, crystallizes from MeOH/EtOAc in the orthorhombic space group *Pbca*. $a = 33.642$ (4), $b = 15.951$ (1), $c = 6.785$ (1) Å, $V = 3641.0$ (4) Å^3, $Z = 8$, $D_x = 1.381$ g cm^{-3}, Cu $K\alpha$, $\lambda = 1.54184$ Å, $\mu = 28.865$ cm^{-1}, $F(000) = 1600$, $T = 223$ K, final R (on F) $= 0.055$ for 1669 observations with $I \geq 3\sigma(I)$. Gly-D,L-Met exists as a cation with the N- and C-termini protonated, the *p*-toluenesulfonate being the counterion. The peptide backbone conformation is a *trans* right-handed helical structure with $\psi_1 = 172.8$ (4), $\omega_1 = -178.9$ (4), $\varphi_2 = -80.6$ (7) and $\psi_2 = -33.8$ (8)°. The methionine residue adopts the $g^-(tg^-)$ conformation. L-His-L-Leu, (III), $C_{12}H_{20}N_4O_3$, $M_r = 268.32$, crystallizes from aqueous ethanol in the monoclinic space group $P2_1$. $a = 6.559$ (1), $b = 5.451$ (1), $c = 20.463$ (2) Å, $\beta = 99.00$ (1)°, $V = 722.7$ (3) Å^3, $Z = 2$, $D_x = 1.233$ g cm^{-3}, Cu $K\alpha$, $\lambda = 1.54184$ Å, $\mu = 7.102$ cm^{-1}, $F(000) = 288$, $T = 295$ K, final R (on F) $= 0.033$ for 1237 observations with $I \geq 3\sigma(I)$. (III) crystallizes as a zwitterion with the N-terminus protonated and the C-terminus ionized. The peptide backbone extends to the C-terminus, which then coils in a helical conformation. Principal torsion angles are $\psi_1 = 164.5$ (2), $\omega_1 = 174.8$ (2), $\varphi_2 = -77.9$ (3) and $\psi_2 = -18.7$ (3)°. The histidyl side chain adopts a *gauche* orientation with the ring twisted slightly from a perpendicular orientation. The leucine residue adopts the $g^-(tg^-)$ conformation. Two intramolecular hydrogen-bonding interactions are proposed, one from the imidazole ring to the ionized C-terminus and the other from the protonated N-terminus to the peptide carbonyl O atom.

Introduction

The positions of amino acids in a peptide sequence and their side-chain bulk and hydrogen-bonding characteristics are factors believed to influence the folding patterns of proteins (Padmanabhan, Marqusee, Ridgeway, Laue & Baldwin, 1990). Conformational studies using crystallographic and

0108-7681/93/010123-08$06.00

theoretical methods (Chandrasekaran, Lakshminarayanan, Pandya & Ramachandran, 1973) show that right-handed helices are preferred by L-amino-acid residues, while sequences incorporating successive LD or DL amino acids favor β bend conformations. Alanine, leucine, methionine and histidine residues are thought to promote right-handed α-helical conformations in proteins, whereas glycine and proline show strong tendencies towards extended strand and bent structures (Fasman, 1989). Recent solution studies of α-helix stabilization by amino-acid residues with alkyl side chains in a series of blocked host peptides suggest that the γ-branded leucine residue has a subtle tendency to destabilize α helices (Lyu, Sherman, Chen & Kallenbach, 1991).

The molecular structures of the unblocked dipeptides, L-Leu-L-Tyr (I), Gly-D,L-Met.*p*-toluenesulfonate (II) and L-His-L-Leu (III), are reported here as part of an ongoing effort in this laboratory to study conformations of linear peptides and the relationship of amino-acid sequence to backbone conformation.

Experimental

Crystals of (I) were obtained as plates from MeOH/5% DMSO (dimethyl sulfoxide), crystals of (II) were obtained as needles or rods from MeOH/EtOAc and needles of (III) (Sigma Chemical Company) were grown from cold aqueous ethanol. For X-ray examination and data collection, suitable crystals of (I) (0.20 × 0.25 × 0.20 mm), (II) (0.20 × 0.50 × 0.08 mm) and (III) (0.70 × 0.15 × 0.02 mm) were individually mounted on the tips of glass fibers with epoxy resin. Intensity data for all of the crystals were collected on an Enraf–Nonius CAD-4 diffractometer system mounted on rotating anode with graphite-monochromatized Cu $K\alpha$ radiation. Lattice parameters were obtained by least-squares refinement of the angular settings for 25 reflections lying in a 2θ range of 60–80°. Intensity data were collected using variable ω–2θ scans in the range $2 \le 2\theta \le 100°$ (1469 reflections) for (I), $2 \le 2\theta \le 135°$ (3271 reflections) for (II) and $2 \le 2\theta \le 135°$ (1495 reflections) for (III). Three standard reflections monitored every 3 h of X-ray exposure time showed a maximum change of +1.3% for (I), −4.5% for (II) and −2.1% for (III). A correction for deterioration was made for (II) and all data were corrected for Lorentz and polarization effects. The data were corrected for absorption using the *DIFABS* algorithm of Walker & Stuart (1983) for (I) (maximum correction 1.094, minimum 0.749) and for (III) (maximum correction 1.211, minimum 0.825). For (II) the absorption correction applied was based on measured ψ scans (maximum transmission correction 99.32%, minimum 87.33%). For (III), symmetry-equivalent reflections ($0kl$, $0k\bar{l}$) were averaged ($R_{int} = 0.017$) to yield the final 1366 unique observations.

The structures were solved by a combination of direct methods, *SHELXS*86 (Sheldrick, 1985) for (I) and (III) *MULTAN*80 (Main, Fiske, Hull, Lessinger, Germain, Declercq & Woolfson, 1980) for (II) and the difference Fourier technique. All structures were refined by full-matrix least-squares calculations (on F). Non-H atoms were first refined with isotropic temperature factors and then, except where noted, with anisotropic displacement parameters. All H-atom positions were located directly from the difference Fourier maps for (I) and refined with fixed isotropic temperature factors. For (II) and (III), most H-atom positions were located directly; those not located thus were calculated with C—H = 1.00 Å, or based on hydrogen-bonding criteria and held fixed with isotropic temperature factors assigned as $1.3B_{eq}$ of the adjacent atom. For (II), large anisotropic displacement parameters at the end of the standard refinement and residual density in a difference Fourier map suggested disorder in the carboxylic acid group. A disorder model that included alternative positions for this group was incorporated, which fixed occupancies at 75% (C2′, O2′, O2″) and 25% (C2′*B*, O2′*B*, O2″*B*) based on a consideration of heights in the difference map and thermal parameters for the refined positions. In the latter stages, the lower occupancy sites were held at fixed positions but isotropic temperature factors for these atoms were refined.

The refinement for (I) converged [$(\Delta/\sigma)_{max} = 0.02$] to values of the standard crystallographic agreement factors of $R = 0.033$, $wR = 0.041$ and $S = 1.964$ for 1347 observations with $I \ge 2\sigma(I)$ and 257 parameters. The refinement for (II) converged [$(\Delta/\sigma)_{max} = 0.02$] with agreement factors $R = 0.055$, $wR = 0.063$ and $S = 1.528$ for 1669 observations with $I \ge 3\sigma(I)$ and 221 parameters. For (III), refinement converged [$(\Delta/\sigma)_{max} = 0.01$] with agreement factors $R = 0.033$, $wR = 0.041$ and $S = 1.569$ for 1237 observations with $I \ge 3\sigma(I)$ and 171 parameters. Weights were assigned to the data as $w = 4F_o^2/\sigma^2(I)$, with $\sigma^2(I)$ defined as $[\sigma(I_c)^2 + (pI)^2]$, $p = 0.02$ for (I), 0.05 for (II) and 0.03 for (III). An extinction coefficient of the form proposed by Zachariasen (1963) was applied and refined: $g = 8.53\ (1) \times 10^{-7}$ for (I) and $g = 1.52\ (1) \times 10^{-7}$ for (II). A final difference Fourier map showed residual electron density of ± 0.203 e Å^{-3} for (I), ± 0.428 e Å^{-3} for (II) and ± 0.186 e Å^{-3} for (III). Using all of the data not marked weak in a prescan, the refinements for (I), (II) and (III) converged to values of the standard crystallographic agreement factors as follows, (I): $R = 0.039$, $wR = 0.043$, $S = 1.952$ for 1419 observations; (II): $R = 0.097$, $wR = 0.078$, $S = 1.315$ for 2691 observations; (III): $R = 0.036$, $wR = 0.042$, $S = 1.546$ for 1329 observations.

Table 1. *Positional parameters and e.s.d.'s for Leu-Tyr*

$B_{eq} = (8\pi^2/3)\sum_i\sum_j U_{ij}a_i^*a_j^*\mathbf{a}_i.\mathbf{a}_j$.

	x	y	z	B_{eq} (Å^2)
O′	0.4466 (4)	0.6222 (2)	0.21906 (8)	2.80 (4)
O″	0.7982 (4)	0.5556 (1)	0.19439 (8)	2.19 (4)
O1	0.3403 (4)	0.2527 (1)	0.16836 (8)	2.34 (4)
O2H	0.2524 (4)	0.2794 (2)	−0.11563 (7)	2.33 (4)
N1	−0.0408 (5)	0.1877 (2)	0.22787 (8)	1.69 (4)
N2	0.2418 (5)	0.4357 (2)	0.16975 (9)	1.57 (4)
C1′	0.2131 (5)	0.3294 (2)	0.1850 (1)	1.54 (5)
C1*A*	0.0140 (5)	0.3083 (2)	0.2291 (1)	1.50 (5)
C1*B*	0.0974 (6)	0.3404 (2)	0.2918 (1)	1.89 (6)
C1*G*	−0.0881 (7)	0.3258 (2)	0.3403 (1)	2.51 (6)
C2′	0.5767 (6)	0.5586 (2)	0.1908 (1)	1.68 (5)
C2*A*	0.4599 (6)	0.4806 (2)	0.1452 (1)	1.57 (5)
C2*B*	0.4136 (6)	0.5459 (2)	0.0875 (1)	1.99 (6)
C2*G*	0.3608 (6)	0.4729 (2)	0.0347 (1)	1.74 (6)
C2*Z*	0.2795 (6)	0.3434 (2)	−0.0655 (1)	1.81 (6)
C1*D*1	0.0288 (8)	0.3320 (3)	0.4009 (1)	4.44 (9)
C1*D*2	−0.2844 (8)	0.4110 (3)	0.3350 (2)	4.54 (9)
C2*D*1	0.1483 (6)	0.4800 (2)	0.0044 (1)	2.03 (6)
C2*D*2	0.5301 (6)	0.3990 (2)	0.0146 (1)	1.84 (5)
C2*E*1	0.1070 (6)	0.4155 (2)	−0.0463 (1)	2.15 (6)
C2*E*2	0.4920 (6)	0.3340 (2)	−0.0356 (1)	1.93 (6)

Table 2. *Positional parameters and e.s.d.'s for Gly-Met.p-toluenesulfonate*

$B_{eq} = (8\pi^2/3)\sum_i\sum_j U_{ij}a_i^*a_j^*\mathbf{a}_i.\mathbf{a}_j$.

	x	y	z	B_{eq} (Å^2)
S1	0.33077 (4)	0.38365 (8)	0.4745 (2)	2.53 (2)
S2*D*	0.44963 (5)	0.6535 (1)	0.4228 (3)	4.89 (4)
O1	0.2716 (1)	0.7133 (3)	0.1666 (6)	4.10 (9)
O2	0.2993 (1)	0.3568 (3)	0.3432 (6)	3.92 (9)
O3	0.3285 (1)	0.4740 (2)	0.5120 (5)	3.58 (8)
O4	0.3329 (1)	0.3357 (2)	0.6555 (5)	3.98 (9)
O2′	0.3233 (2)	0.5325 (3)	−0.1134 (8)	4.7 (1)
O2′*B*	0.350	0.580	−0.220	2.5 (3)†
O2″*B*	0.310	0.520	−0.035	3.8 (3)†
O2″	0.3469 (2)	0.6443 (3)	−0.2623 (7)	5.0 (1)
N1	0.2227 (1)	0.6780 (3)	0.4625 (6)	2.89 (9)
N2	0.3181 (1)	0.6177 (3)	0.2465 (6)	2.93 (9)
C1	0.3761 (2)	0.3685 (3)	0.348[illegible] (8)	2.5 (1)
C1′	0.2829 (2)	0.6556 (3)	0.2695 (7)	2.5 (1)
C1*A*	0.2576 (2)	0.6237 (3)	0.4415 (8)	3.0 (1)
C2*A*	0.3452 (2)	0.6427 (3)	0.0971 (8)	2.9 (1)
C2	0.4090 (2)	0.3373 (3)	0.4486 (9)	3.2 (1)
C2′	0.3383 (2)	0.6099 (5)	−0.117 (1)	3.4 (2)
C2*B*	0.3883 (2)	0.6242 (4)	0.1560 (8)	3.3 (1)
C2*G*	0.4012 (2)	0.6785 (4)	0.3259 (9)	3.5 (1)
C2*E*	0.4401 (2)	0.5558 (5)	0.538 (1)	6.5 (2)
C2′*B*	0.330	0.580	−0.061	2.2 (3)†
C3	0.4451 (2)	0.3349 (4)	0.346 (1)	4.5 (2)
C4	0.4489 (2)	0.3628 (4)	0.157 (1)	4.1 (1)
C5	0.4150 (2)	0.3899 (4)	0.0554 (9)	3.8 (1)
C6	0.3790 (2)	0.3932 (3)	0.1541 (9)	3.4 (1)
C7	0.4888 (2)	0.3633 (5)	0.052 (1)	6.0 (2)

† Atom refined isotropically.

Table 3. *Positional parameters and e.s.d.'s for His-Leu*

$B_{eq} = (8\pi^2/3)\sum_i\sum_j U_{ij}a_i^*a_j^*\mathbf{a}_i.\mathbf{a}_j$.

	x	y	z	B_{eq} (Å^2)
O″	0.8246 (3)	−0.454	0.83070 (8)	2.65 (4)
O′	0.7914 (3)	−0.1448 (4)	0.75862 (9)	2.65 (4)
O1	1.3408 (3)	−0.5103 (4)	0.79522 (9)	3.02 (4)
N1*D*	1.1256 (3)	−0.6085 (5)	0.92826 (9)	1.99 (4)
N1	1.5626 (3)	−0.9005 (4)	0.84192 (9)	1.97 (4)
N1*E*	1.2759 (3)	−0.6082 (5)	1.03286 (9)	2.16 (4)
N2	1.0535 (3)	−0.7255 (5)	0.7554 (1)	2.22 (4)
C1*B*	1.2343 (3)	−1.0104 (5)	0.8835 (1)	1.86 (5)
C1*E*	1.1528 (3)	−0.4867 (6)	0.9865 (1)	2.00 (5)
C1*D*	1.3292 (3)	−0.8193 (5)	1.0020 (1)	1.95 (5)
C1*G*	1.2381 (3)	−0.8212 (5)	0.9368 (1)	1.74 (4)
C1′	1.2441 (3)	−0.7025 (5)	0.7894 (1)	1.82 (4)
C1*A*	1.3358 (3)	−0.9379 (5)	0.8229 (1)	1.73 (4)
C2*A*	0.9389 (4)	−0.5138 (6)	0.7254 (1)	2.24 (5)
C2*D*1	0.6501 (9)	−0.837 (1)	0.5676 (2)	12.0 (2)
C2′	0.8452 (3)	−0.3602 (5)	0.7763 (1)	1.94 (5)
C2*D*2	0.971 (1)	−0.585 (2)	0.5781 (2)	15.1 (2)
C2*G*	0.8365 (7)	−0.741 (1)	0.6147 (2)	6.41 (1)
C2*B*	0.7651 (5)	−0.5992 (7)	0.6718 (1)	3.65 (6)

Scattering factors were taken from *International Tables for X-ray Crystallography* (1974, Vol. IV) except for the H atoms [from Stewart, Davidson & Simpson (1965)]. The effects of anomalous dispersion for non-H atoms were included. All programs used were from the locally modified Enraf–Nonius (1979) structure determination package (*SDP*). Positional parameters and equivalent isotropic temperature factors for (I), (II) and (III) are given in Tables 1, 2 and 3, respectively.*

Discussion

The molecular structures of (I), (II) and (III) are shown in Figs. 1, 2 and 3, respectively, while their packing diagrams are shown in Figs. 4, 5 and 6, respectively. Principal bond distances and bond angles for (I), (II) and (III) are collected in Tables 4, 5 and 6, respectively. Principal torsion angles as defined by the IUPAC–IUB Commission on Biochemical Nomenclature (1970) are listed in Table 7. Hydrogen-bonding interactions are given in Table 8.

L-*Leu*-L-*Tyr* (I)

(I) crystallizes as a zwitterion with ionized C-terminus and protonated N-terminus. The peptide bond adopts a distorted *trans* conformation with ω_1 [158.7 (2)°] being 21.3° out of the plane in comparison to the fully extended value of 180°. Similar large distortions from the ideal in peptide bonds have often been observed; in the structure of glutamyl-aspartic acid (Eggleston & Hodgson, 1985) a 19° distortion was found, in the N-terminal tetrapeptide from angiotensin II (Feldman & Eggleston, 1990) two of the three peptide bonds are distorted by 12° or more, and in a blocked form of the sequence glycyl-glycyl-tyrosine (Krause & Eggleston, 1992) the peptide bond between glycine and tyrosine is also distorted. These distortions are invariably accompanied by hydrogen-bonding interactions involving the amide functionality; often strong intermolecular interactions with the carbonyl oxygen, as in the current structure (*vide infra*) are observed. Since out-of-plane amide bond deformations of the order of 10–20° require expenditure of only a few

* Lists of structure factors, anisotropic thermal parameters and H-atom parameters have been deposited with the British Library Document Supply Centre as Supplementary Publication No. SUP 55578 (42 pp.). Copies may be obtained through The Technical Editor, International Union of Crystallography, 5 Abbey Square, Chester CH1 2HU, England. [CIF refereence: CD0063].

kJ mol^{-1} of energy (Dunitz & Winkler, 1975) distortions of this nature clearly may be induced and compensated for by strong intermolecular interactions in the crystalline environment.

The torsion angles $\varphi_2 = -110.9\,(3)$ and $\psi_2 = 141.4\,(2)^\circ$ describe an antiparallel β pleated sheet, for which typical values are $\varphi = -140$ and $\psi = 135^\circ$ (Arnott, Dover & Elliott, 1967). The φ and ψ values are quite similar to those found in molecule *B* of the related blocked dipeptide, Ac-Leu-Tyr-OMe (Karle & Flippen-Anderson, 1989). The leucyl residue adopts the $g^-(tg^-)$ conformation (Benedetti, Morelli, Nemethy & Scheraga, 1983), where $\chi^1 = -63.7\,(3)^\circ$ and the $\chi^{2,1}$ and $\chi^{2,2}$ angles are 166.0 (2) and $-70.8\,(3)^\circ$, respectively. The tyrosine residue adopts the g^- [$\chi^1 = -74.2\,(3)^\circ$] conformation. The aromatic ring is twisted away [$\chi^{2,1} = -62.4\,(4)$ and $\chi^{2,2} = 119.6\,(3)^\circ$] from a perpendicular orientation ($\chi^2 = \pm 90^\circ$).

Quite remarkably, examination of the peptides of known structure which contain the -Leu-Tyr- sequence (Table 7) indicates that in seven out of nine observations, the conformation adopted is the anti-

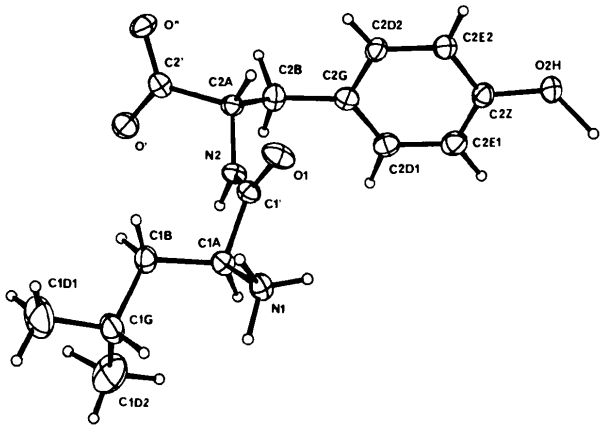

Fig. 1. Labeled drawing of Leu-Tyr showing 50% thermal-ellipsoid probability for the non-H atoms, H atoms as small spheres of arbitrary size.

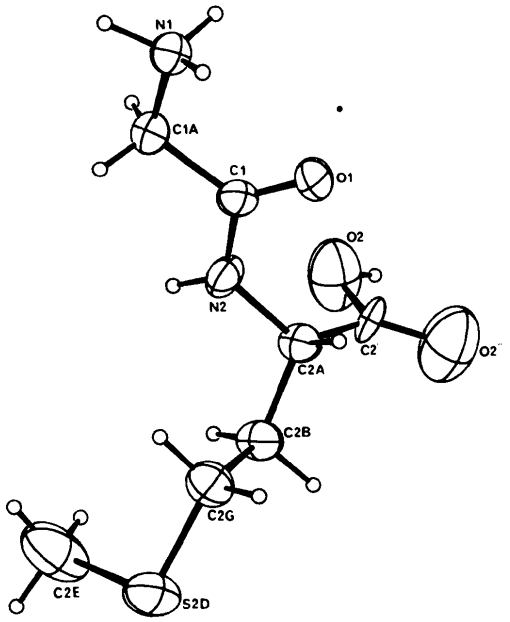

Fig. 2. Labeled drawing of Gly-D,L-Met.*p*-toluenesulfonate showing 50% thermal-ellipsoid probability for the non-H atoms, H atoms as small spheres of arbitrary size. Atoms of the disordered C-terminus are shown in their positions of highest occupancy.

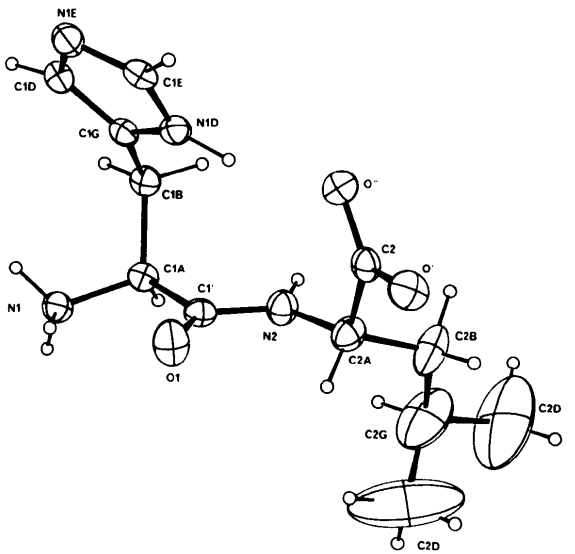

Fig. 3. Labeled drawing of His-Leu showing 50% thermal-ellipsoid probability for the non-H atoms, H atoms as small spheres of arbitrary size.

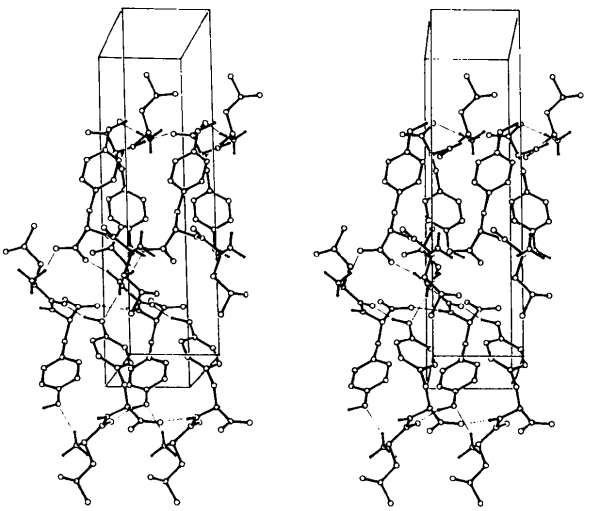

Fig. 4. Stereo packing diagram of Leu-Tyr indicating hydrogen bonding. Hydrogen-bonding interactions are indicated by thin lines. The *a* axis runs horizontally and the *c* axis runs vertically.

Table 4. *Selected bond distances* (Å) *and angles* (°) *for Leu-Tyr* (*e.s.d.'s in parentheses*)

O′—C2′	1.239 (3)	C1*G*—C1*D*2	1.518 (4)
O″—C2′	1.254 (3)	C2′—C2*A*	1.543 (3)
O1—C1′	1.231 (2)	C2*A*—C2*B*	1.545 (3)
O2*H*—C2*Z*	1.378 (2)	C2*B*—C2*G*	1.510 (3)
N1—C1*A*	1.490 (2)	C2*G*—C2*D*1	1.383 (3)
N2—C1′	1.341 (2)	C2*G*—C2*D*2	1.386 (3)
N2—C2*A*	1.455 (3)	C2*Z*—C2*E*1	1.377 (3)
C1′—C1*A*	1.522 (3)	C2*Z*—C2*E*2	1.381 (3)
C1*A*—C1*B*	1.538 (3)	C2*D*1—C2*E*1	1.404 (3)
C1*B*—C1*G*	1.526 (3)	C2*D*2—C2*E*2	1.393 (3)
C1*G*—C1*D*1	1.518 (3)		

C1′—N2—C2*A*	123.9 (2)	N2—C2*A*—C2′	109.7 (2)
O1—C1′—N2	124.9 (2)	N2—C2*A*—C2*B*	111.6 (2)
O1—C1′—C1*A*	120.3 (2)	C2′—C2*A*—C2*B*	108.7 (2)
N2—C1′—C1*A*	114.7 (2)	C2*A*—C2*B*—C2*G*	113.5 (2)
N1—C1*A*—C1′	107.7 (2)	C2*B*—C2*G*—C2*D*1	121.7 (2)
N1—C1*A*—C1*B*	109.1 (2)	C2*B*—C2*G*—C2*D*2	119.9 (2)
C1′—C1*A*—C1*B*	109.4 (2)	C2*D*1—C2*G*—C2*D*2	118.4 (2)
C1*A*—C1*B*—C1*G*	114.8 (2)	O2H—C2*Z*—C2*E*1	122.3 (2)
C1*B*—C1*G*—C1*D*1	110.0 (2)	O2H—C2*Z*—C2*E*2	116.8 (2)
C1*B*—C1*G*—C1*D*2	111.4 (2)	C2*E*1—C2*Z*—C2*E*2	120.8 (2)
C1*D*1—C1*G*—C1*D*2	110.8 (2)	C2*G*—C2*D*1—C2*E*1	120.9 (2)
O′—C2′—O″	125.2 (2)	C2*G*—C2*D*2—C2*E*2	121.6 (2)
O′—C2′—C2*A*	117.9 (2)	C2*Z*—C2*E*1—C2*D*1	119.4 (2)
O″—C2′—C2*A*	116.8 (2)	C2*Z*—C2*E*2—C2*D*2	119.0 (2)

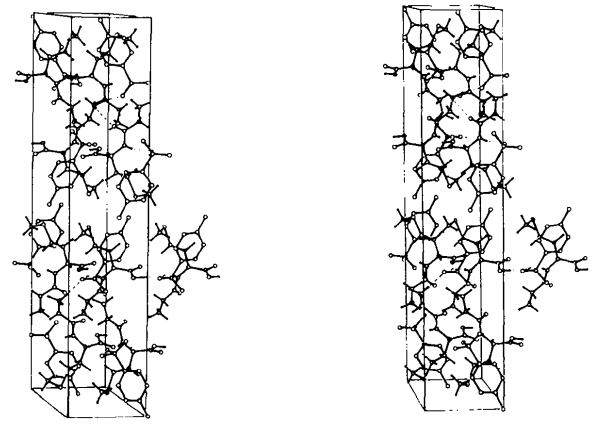

Fig. 5. Stereo packing diagram of Gly-D,L-Met.*p*-toluenesulfonate indicating hydrogen bonding. Hydrogen-bonding interactions are indicated by dashed lines. The *a* axis runs vertically and the *c* axis runs horizontally.

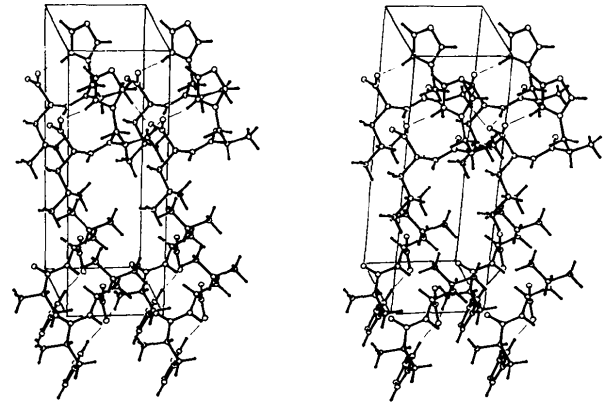

Fig. 6. Stereo packing diagram of His-Leu indicating hydrogen bonding. Hydrogen-bonding interactions are indicated by thin lines. The *a* axis runs horizontally while the *c* axis runs vertically.

Table 5. *Bond distances* (Å) *and angles* (°) *for Gly-Met.p-toluenesulfonate* (*e.s.d.'s in parentheses*)

S1—O2	1.449 (3)	N1—C1*A*	1.467 (5)
S1—O3	1.465 (3)	N2—C1′	1.340 (5)
S1—O4	1.449 (3)	N2—C2*A*	1.445 (5)
S1—C1	1.766 (5)	C1′—C1*A*	1.530 (6)
S2*D*—C2*G*	1.801 (5)	O2′*B*—C2′*B*	1.266
S2*D*—C2*E*	1.773 (6)	C2*A*—C2*B*	1.540 (6)
O1—C1′	1.216 (5)	C2*A*—C2′*B*	1.533
C1—C2	1.389 (6)	C2*B*—C2*G*	1.507 (6)
O2′—C2′	1.336 (8)	C3—C4	1.361 (8)
C2*A*—C2′	1.531 (8)	C4—C5	1.400 (7)
O2″*B*—C2′*B*	1.182	C4—C7	1.520 (7)
O2″—C2′	1.164 (8)	C5—C6	1.388 (6)
C2—C3	1.403 (7)	C1—C6	1.381 (6)

O2—S1—O3	111.0 (2)	S1—C1—C6	118.8 (4)
O2—S1—O4	113.6 (2)	C2—C1—C6	121.0 (5)
O2—S1—C1	107.1 (2)	O1—C1′—N2	123.4 (4)
O3—S1—O4	112.0 (2)	N2—C2*A*—C2*B*	109.6 (4)
O1—C1′—C1*A*	121.1 (4)	N2—C2*A*—C2′*B*	95.9
N2—C1′—C1*A*	115.5 (4)	C2′—C2*A*—C2*B*	109.7 (4)
N1—C1*A*—C1′	108.8 (4)	C1—C2—C3	117.1 (5)
N2—C2*A*—C2′	118.9 (4)	O2′—C2′—O2″	123.1 (7)
C2*A*—C2*B*—C2*G*	112.1 (4)	O2′—C2′—C2*A*	110.8 (6)
S2*D*—C2*G*—C2*B*	114.4 (3)	O2″—C2′—C2*A*	125.9 (6)
O2′*B*—C2′*B*—O2″*B*	115.3	O2″*B*—C2′*B*—C2*A*	128.0
O2′*B*—C2′*B*—C2*A*	113.7	C2—C3—C4	122.7 (5)
O3—S1—C1	105.3 (2)	C3—C4—C5	119.2 (5)
O4—S1—C1	107.2 (2)	C3—C4—C7	121.7 (6)
C2*G*—S2*D*—C2*E*	101.1 (3)	C5—C4—C7	119.1 (6)
C2*B*—C2*A*—C2′*B*	112.3	C4—C5—C6	119.1 (5)
C1′—N2—C2*A*	121.2 (4)	C1—C6—C5	120.7 (5)
S1—C1—C2	120.0 (4)		

Table 6. *Selected bond distances* (Å) *and angles* (°) *for His-Leu* (*e.s.d.'s in parentheses*)

O″—C2′	1.251 (3)	C1*B*—C1*G*	1.498 (4)
O′—C2′	1.263 (3)	C1*B*—C1*A*	1.548 (3)
O1—C1′	1.221 (3)	C1*D*—C1*G*	1.375 (3)
N1*D*—C1*E*	1.351 (3)	C1′—C1*A*	1.532 (4)
N1*D*—C1*G*	1.371 (3)	C2*A*—C2′	1.538 (4)
N1—C1*A*	1.491 (3)	C2*A*—C2*B*	1.526 (4)
N1*E*—C1*E*	1.324 (3)	C2*D*1—C2*G*	1.527 (7)
N1*E*—C1*D*	1.383 (4)	C2*D*2—C2*G*	1.505 (9)
N2—C1′	1.338 (3)	C2*G*—C2*B*	1.533 (5)
N2—C2*A*	1.459 (4)		

C1*E*—N1*D*—C1*G*	108.0 (2)	N1—C1*A*—C1′	108.0 (2)
C1*E*—N1*E*—C1*D*	105.0 (2)	C1*B*—C1*A*—C1′	112.5 (2)
C1′—N2—C2*A*	121.5 (2)	N2—C2*A*—C2′	112.4 (2)
C1*G*—C1*B*—C1*A*	116.6 (2)	N2—C2*A*—C2*B*	109.8 (2)
N1*D*—C1*E*—N1*E*	111.6 (2)	C2′—C2*A*—C2*B*	108.7 (2)
N1*E*—C1*D*—C1*G*	110.3 (2)	O″—C2′—O′	124.9 (2)
N1*D*—C1*G*—C1*B*	122.9 (2)	O″—C2′—C2*A*	119.3 (2)
N1*D*—C1*G*—C1*D*	105.1 (2)	O′—C2′—C2*A*	115.8 (2)
C1*B*—C1*G*—C1*D*	131.8 (2)	C2*D*1—C2*G*—C2*D*2	110.8 (4)
O1—C1′—N2	124.0 (2)	C2*D*1—C2*G*—C2*B*	110.1 (4)
O1—C1′—C1*A*	120.9 (2)	C2*D*2—C2*G*—C2*B*	111.7 (5)
N2—C1′—C1*A*	115.1 (2)	C2*A*—C2*B*—C2*G*	114.8 (3)
N1—C1*A*—C1*B*	111.2 (2)		

parallel β sheet. The preference for the sheet conformation in peptides containing Leu-Tyr is consistent with observations that the leucyl residue may exert a subtle influence in destabilizing α-helices (Lyu, Sherman, Chen & Kallenbach, 1991) and with observations that amino-acid residues with restricted side-chain rotamer conformations may also influence helix-forming tendency (Padmanabhan, Marqusee, Ridgeway, Laue & Baldwin, 1990). However, in at least two instances a helical-type conformation has been observed for the Leu-Tyr sequence in short peptides, so its γ branching does not totally exclude the ability to form structures in the helical region.

Table 7. *Principal torsion angles* (°) *and backbone conformations of selected linear peptides containing Leu-Tyr, Met or His*

L residues except where specifically denoted otherwise. In structures with multiple independent molecules, molecule *B* is on the second line and molecule *C* is on the third line.

Peptide*	φ_1	ψ_1	ω_1	φ_2	ψ_2	ω_2	φ_3	ψ_3	Conformation
Leu-Tyr[a]		164	159	−101	141				Antiparallel β sheet
Gly-Leu-Tyr[b,c]		170	177	−131	148	174	−146	169	Antiparallel β sheet
		154	−179	−146	134	176	−140	171	Antiparallel β sheet
Leu-Tyr-Leu[d]		162	−177	−130	121	−174	−114	159	Antiparallel β sheet
		125	175	−83	137	173	−134	140	Antiparallel β sheet
Leu-Leu-Tyr[e]		120	−177	−101	−53	−174	−88		Right helical
Ac-Leu-Tyr-OMe[f]	−70	−48	176	−100	167	177			Antiparallel β sheet
	−81	−25	171	−103	148	−178			Antiparallel β sheet
	−55	−44	−175	−109	−17	176			Type I β turn
Gly-D,L-Met[g]		173	−179	−81	−34				Right helical
Pro-Met[g]		166	168	−71	−29				Right helical
Boc-Pro-Met-OBzl[h]		174	−179	−138	140				Antiparallel β sheet
		174	−176	−134	136				Antiparallel β sheet
Met-Met[i]		133	180	−149	173				Antiparallel β sheet
Boc-D-Met-Met-OMe[j]	72	−74	−171	−65	38				γ turn
D,L-Ala-L,D-Met[k]		152	172	152	−176				Inverse antiparallel β sheet
Boc-Met-Gly-OBzl[l]	−111	108							Parallel β sheet
Boc-Met-Gly-OEt[m]	−119	115							Parallel β sheet
Trp-Met-Asp-Phe-NH_2[n]		157	167	−133	164	180			Antiparallel β sheet
		140	173	−145	158	174			Antiparallel β sheet
His-Leu[o]		165	175	−80	−19				Right helical
Hip-His-Leu[o]	−67	141	171	−157	163	175	−97		Antiparallel β sheet
D,L-His-L,D-His[p]		162	177	−152	157				Antiparallel β sheet
TRH[q]		146		−70	137			153	Antiparallel β sheet
His-Ser[r]		128	174	−136					Antiparallel β sheet
Met-Glu-His-Phe[s]						−177	−172	171	Fully extended

References: (*a*) this work; (*b*) Subramanian & Parthasarathy (1987); (*c*) Wu, Tinant, Declercq & van Meerssche (1987); (*d*) Wu, Declercq, Tinant & van Meerssche (1987); (*e*) Delettre, Berthou, Lifchitz & Jolles (1988); (*f*) Karle & Flippen-Anderson (1989); (*g*) Padmanabhan & Yadava (1983); (*h*) Yamane, Shiraishi & Ashida (1985); (*i*) Stenkamp & Jensen (1975); (*j*) Immirzi, Avena, Ciajolo, Becker & Naider (1978); (*k*) Stenkamp & Jensen (1974); (*l*) Yamane, Umemura, Kojima, Yamada & Ashida (1980); (*m*) Youwei, Yicheng & Yougi (1985); (*n*) Cruse, Egert, Viswamitra & Kennard (1982); (*o*) Vrielink & Codding (1985); (*p*) Krause & Eggleston (1991); (*q*) Kamiya, Takamoto, Wada, Fujino & Niskhikawa (1980); (*r*) Suresh & Vijayan (1985); (*s*) Admiraal & Vos (1983).

* Torsion angles correspond to Leu-Tyr, Met or His residues only.

Intermolecular hydrogen bonding (Table 8 and Fig. 4) links molecules in a head-to-tail fashion with the protonated N-terminus interacting with the ionized C-terminus (N1···O′ and N1···O″). In addition, the N-terminus participates in a rather bent hydrogen bond with the side chain of the tyrosine residue (N1···O2H). The amide N atom, N2, interacts with the C-terminus oxygen, O″, while the hydroxyl oxygen, O2H, interacts, very strongly by distance criteria, with the carbonyl oxygen, O1. In the structure of α-glutamyl-glutamic acid, another peptide displaying a distorted *trans* amide bond (Eggleston & Hodgson, 1982), a similar combination of intermolecular hydrogen-bonding interactions is observed with a tight link (2.713 Å) between a hydroxyl donor from a glutamic acid side chain and the peptide carbonyl oxygen. A strong similarity in hydrogen-bonding interactions to the peptide carbonyl oxygen in (I) is also observed in the structure of Z-Gly-Gly-Tyr-OMe (Krause & Eggleston, 1992). In (I), as in that other structure, a tight tyrosine OH···O interaction is observed with a separation of only 2.6 Å between oxygens. This distance is comparable to those normally observed in carboxylic acid dimers and, combined with the near linearity at hydrogen (Taylor & Kennard, 1984), may indicate a very strong directional influence at the amide carbonyl. These observations are suggestive of a general pattern for hydrogen-bond-imposed peptide-bond distortions in larger peptide (protein) structures, but current refinement methods in macromolecular crystallography would mask such effects by constraining peptide bonds to ideal values for the convenience of reducing the number of variables in refinement of large structures with low data-to-variable ratios (Sussman, 1985).

Gly-D,L-*Met.p-toluenesulfonate* (II)

Gly-D,L-Met exists as a cation with the N- and C-termini protonated, the *p*-toluenesulfonate being the counterion. The peptide backbone adopts a *trans* right-handed helical conformation with $\omega_1 = -178.9\,(4)$, $\varphi_2 = -80.6\,(7)$ and $\psi_2 = -33.8\,(8)°$. Theoretical values for a 3_{10}-helical structure are $\varphi = -60$ and $\psi = -30°$ (Ramachandran & Sasisekharan, 1968). The methionine residue adopts the $g^-(tg^-)$ conformation where χ^1, χ^2 and χ^3 are $-67.0\,(6)$, $174.6\,(4)$ and $-70.4\,(5)°$, respectively. This is the most commonly observed methionyl-residue side-chain conformation.

Conformational studies (Chandrasekaran, Lakshminarayanan, Pandya & Ramachandran, 1973) suggest that structures containing LD or DL sequences tend to favor a β turn conformation, but in this study a helical structure in the 3_{10} region is

Table 8. *Hydrogen-bonding interactions* (Å, °)

D—H···*A*	*D*—*A*	H···*A*	*D*—H···*A*	Symmetry code
Leu-Tyr				
N1—H1···O''	2.739 (3)	1.72 (3)	155 (2)	(i)
N1—H2···O'	2.703 (3)	1.77 (6)	174 (3)	(ii)
N1—H3···O2H	2.815 (2)	2.10 (4)	133 (4)	(iii)
N2—H5···O''	2.946 (3)	2.05 (5)	163 (3)	(iv)
O2H—H20···O1	2.641 (2)	1.58 (6)	167 (7)	(iii)
Gly-Met				
N1—H1···O1	2.763 (5)	2.24	124	(v)
N1—H1···O2	3.050 (8)	2.28	142	(vi)
N1—H2···O4	2.805 (5)	1.92	175	(vii)
N1—H3···O2	2.744 (5)	1.75	168	(viii)
N2—H6···O3	2.938 (5)	2.10	167	(ix)
O2'—H8···O3	2.713 (5)	1.80	179	(x)
His-Leu				
N1—H1···O'	2.783 (3)	1.83	172	(xi)
N1—H2···N1*E*	2.850 (3)	1.91	177	(xii)
N1—H3···O1	2.668 (3)	2.20	112	(ix)
N1—H3···O''	3.008 (2)	2.21	151	(iv)
N2—H10···O'	2.867 (3)	1.90	166	(xiii)
N1*D*—H7···O''	2.712 (2)	1.79	164	(ix)

Symmetry code: (i) $1-x, \frac{1}{2}+y, \frac{1}{2}-z$; (ii) $-x, \frac{1}{2}+y, \frac{1}{2}-z$; (iii) $\frac{1}{2}+x, \frac{1}{2}-y, -z$; (iv) $1-x, y, z$; (v) $x, \frac{1}{2}+y, \frac{1}{2}-z$; (vi) $\frac{1}{2}-x, \frac{1}{2}+y, \frac{1}{2}+z$; (vii) $\frac{1}{2}-x, 1-y, \frac{1}{2}-z$; (viii) $\frac{1}{2}-x, 1-y, \frac{1}{2}+z$; (ix) x, y, z; (x) $x, y, z-1$; (xi) $1-x, 1+y, z$; (xii) $3-x, y-\frac{1}{2}, 2-z$; (xiii) $x, 1+y, z$.

observed. A survey (Table 7) of several linear methionine-containing peptide structures reveals that the β sheet (either parallel or antiparallel) is a common conformation adopted through the methionyl residue. As with the -Leu-Tyr- peptides, while helical and turn structures are also adoped, in eight out of ten examples a sheet-type structure is observed, suggesting that the role of side-chain branching may be less definitive than is implied by Leu peptides in determining backbone conformations, at least in small peptide sequences.

Intermolecular hydrogen bonding (Table 8 and Fig. 5) occurs between the protonated N-terminus and the *p*-toluenesulfonate counterion. One of the N-terminal H atoms also participates in a three-center interaction involving the symmetry-related amide carbonyl oxygen, O1. As a result of the hydrogen-bonding interactions, the unit cell is comprised of chains with the Gly-Met and *p*-toluenesulfonate molecules in alternating rows along the *a* axis.

L-*His*-L-*Leu* (III)

The structure of (III) shows a zwitterionic molecule, ionized at the carboxyl terminus and protonated at the amino terminus. The peptide backbone adopts a fully extended *trans* right-handed helical conformation [$\omega_1 = 174.8$ (2), $\varphi_2 = -78.1$ (3) and $\psi_2 = -18.7$ (3)°], also in the 3_{10} region of a Ramachandran map. The carboxylate orientation is accompanied by an intramolecular hydrogen bond to the histidyl residue with histidyl nitrogen, N1*D*, acting as the donor to O''. The ten-membered ring thus formed is similar in conformational character to a β-turn or the reverse of an Asx turn (Abbadi, Mcharfi, Aubry, Premilat, Boussard & Marraud, 1991), in which the histidyl side chain (donor) plays a role analogous to Asn or Asp (acceptor) in the latter. Indeed, the φ/ψ angles for the leucine residue in this peptide structure ($-78/-19°$) are remarkably similar to values for the type-II-*g* Asx turns calculated by Abbadi *et al.* (1991). Furthermore, this intramolecular hydrogen-bonding motif is common among structurally characterized histidyl peptides. For instance, in the structure of the C-terminal amide of TRH (thyrotropin-releasing hormone), histidyl forms an intramolecular hydrogen bond to the terminal amide carbonyl oxygen (Kamiya, Takamoto, Wada, Fujino & Nishikawa, 1980). Similarly, in three other structures; Hip-His-Leu (Vrielink & Codding, 1985), a histidyl-serine complex (Suresh & Vijayan, 1985) and a fragment of ACTH (adrenocorticotropic hormone; Met-Glu-His-Phe; Admiraal & Vos, 1983), the histidyl residue intramolecularly hydrogen bonds to an ionized C-terminal carboxylate oxygen. Formation of an intramolecular hydrogen bond from one histidyl ring to a second adjacent histidyl ring has also been observed in the structure of DL-His-LD-His (Krause & Eggleston, 1991).

In (III), the histidyl side-chain conformation, with $\chi^2 = 65.1$ (3), $\chi^{2,1} = 69.1$ (3)°, is undoubtedly influenced by formation of the intramolecular interaction and is remarkably similar to that seen in other structures that contain analogous intramolecular hydrogen bonding. The leucine residue adopts the energetically preferred $g^-(tg^-)$ conformation with $\chi^1 = -60.7$ (3) and $\chi^{2,1} = 174.7$ (4), $\chi^{2,2} = -61.8$ (5)°.

Additional intermolecular hydrogen bonding (Table 8 and Fig. 6) is seen between the N-terminus and the carboxylate, between the amide nitrogen and the carboxylate, and between the N-terminus and the imidazole ring. The peptide carbonyl oxygen, O1, is not involved in the hydrogen-bonding scheme intermolecularly, but atom H3 appears to interact with this O atom intramolecularly to form a C5-type structure.

While the database of linear His-containing peptides is smaller than that of molecules containing other residues, the predominant observation in these short sequences is of extended structures. The His-Leu structure provides an additional example of a way in which functionalized side chains can influence a peptide-backbone conformation. Observation of similar intramolecular interactions in a number of histidyl-containing peptide crystal structures emphasizes their potential importance, particularly in short sequences.

The authors thank Dr K. Kopple (SmithKline Beecham Pharmaceuticals) for peptide samples (I) and (II). This work was supported in part by Grant

No. GM39S26-02 from the National Institutes of Health. JAK thanks the NIH for postdoctoral support under this grant.

References

ABBADI, A., MCHARFI, M., AUBRY, A., PREMILAT, S., BOUSSARD, G. & MARRAUD, M. (1991). *J. Am. Chem. Soc.* **113**, 2729–2735.

ADMIRAAL, G. & VOS, A. (1983). *Acta Cryst.* C**39**, 82–87.

ARNOTT, S., DOVER, S. D. & ELLIOTT, A. (1967). *J. Mol. Biol.* **30**, 201–208.

BENEDETTI, E., MORELLI, G., NEMETHY, G. & SCHERAGA, H. A. (1983). *Int. J. Pept. Protein Res.* **22**, 1–15.

CHANDRASEKARAN, R., LAKSHMINARAYANAN, A. V., PANDYA, U. V. & RAMACHANDRAN, G. N. (1973). *Biochim. Biophys. Acta*, **303**, 14–27.

CRUSE, W. B. T., EGERT, E., VISWAMITRA, M. A. & KENNARD, O. (1982). *Acta Cryst.* B**38**, 1758–1764.

DELETTRE, J., BERTHOU, J., LIFCHITZ, A. & JOLLES, P. (1988). *Acta Cryst.* C**44**, 905–907.

DUNITZ, J. D. & WINKLER, F. K. (1975). *Acta Cryst.* B**31**, 251–263.

EGGLESTON, D. S. & HODGSON, D. J. (1982). *Acta Cryst.* B**38**, 1216–1220.

EGGLESTON, D. S. & HODGSON, D. J. (1985). *Int. J. Pept. Protein Res.* **26**, 509–517.

Enraf–Nonius (1979). *Structure Determination Package*. Enraf–Nonius, Delft, The Netherlands.

FASMAN, G. D. (1989). *Prediction of Protein Structures and the Principles of Protein Conformations*, edited by G. D. FASMAN, pp. 193–301. New York: Plenum Press.

FELDMAN, S. H. & EGGLESTON, D. S. (1990). *Acta Cryst.* C**46**, 678–682.

IMMIRZI, A., AVENA, P., CIAJOLO, M. R., BECKER, J. M. & NAIDER, F. (1978). *Acta Cryst.* B**34**, 179–183.

IUPAC–IUB COMMISSION ON BIOCHEMICAL NOMENCLATURE (1970). *J. Mol. Biol.* **52**, 1–17.

KAMIYA, K., TAKAMOTO, M., WADA, Y., FUJINO, M. & NISHIKAWA, M. (1980). *J. Chem. Soc. Chem. Commun.* pp. 438–439.

KARLE, I. L. & FLIPPEN-ANDERSON, J. L. (1989). *Acta Cryst.* C**45**, 791–795.

KRAUSE, J. A. & EGGLESTON, D. S. (1991). *Acta Cryst.* B**47**, 506–511.

KRAUSE, J. A. & EGGLESTON, D. S. (1992). *Int. J. Pept. Protein Res.* In the press.

LYU, P. C., SHERMAN, J. C., CHEN, A. & KALLENBACH, N. R. (1991). *Proc. Natl Acad. Sci. USA*, **88**, 5317–5320.

MAIN, P., FISKE, S. J., HULL, S. E., LESSINGER, L., GERMAIN, G., DECLERCQ, J.-P. & WOOLFSON, M. M. (1980). *MULTAN*80. *A System of Computer Programs for the Automatic Solution of Crystal Structures from X-ray Diffraction Data*. Univs. of York, England, and Louvain, Belgium.

PADMANABHAN, S., MARQUSEE, S., RIDGEWAY, T., LAUE, T. M. & BALDWIN, R. L. (1990). *Nature (London)*, **344**, 268–270.

PADMANABHAN, V. M. & YADAVA, V. S. (1983). *Curr. Sci.* **52**, 904–906.

RAMACHANDRAN, G. N. & SASISEKHARAN, V. (1968). *Adv. Protein Chem.* **23**, 283–437.

SHELDRICK, G. M. (1985). *SHELXS*86. In *Crystallographic Computing* 3, edited by G. M. SHELDRICK, C. KRÜGER & R. GODDARD, pp. 175–189. Oxford Univ. Press.

STENKAMP, R. E. & JENSEN, L. H. (1974). *Acta Cryst.* B**30**, 1541–1545.

STENKAMP, R. E. & JENSEN, L. H. (1975). *Acta Cryst.* B**31**, 857–861.

STEWART, R. F., DAVIDSON, E. R. & SIMPSON, W. T. (1965). *J. Chem. Phys.* **42**, 3176–3187.

SUBRAMANIAN, E. & PARTHASARATHY, R. (1987). *Curr. Sci.* **56**, 1210–1213.

SURESH, C. G. & VIJAYAN, M. (1985). *Int. J. Pept. Protein Res.* **26**, 329–336.

SUSSMAN, J. L. (1985). *Methods Enzymol.* **115**, 271–303.

TAYLOR, R. A. & KENNARD, O. (1984). *Acc. Chem. Res.* **17**, 320–326.

VRIELINK, A. & CODDING, P. W. (1985). *Proc. Am. Crystallogr. Assoc. Winter Meet. Abstr.* **13**, 66.

WALKER, N. & STUART, D. (1983). *Acta Cryst.* A**39**, 158–166.

WU, S., DECLERCQ, J.-P., TINANT, B. & VAN MEERSSCHE, M. (1987). *Bull. Soc. Chim. Belg.* **96**, 525–530.

WU, S., TINANT, B., DECLERCQ, J.-P. & VAN MEERSSCHE, M. (1987). *Bull. Soc. Chim. Belg.* **96**, 367–372.

YAMANE, T., SHIRAISHI, Y. & ASHIDA, T. (1985). *Acta Cryst.* C**41**, 946–950.

YAMANE, T., UMEMURA, T., KOJIMA, T., YAMADA, Y. & ASHIDA, T. (1980). *Bull. Chem. Soc. Jpn*, **53**, 908–912.

YOUWEI, Y., YICHENG, D. & YOUGI, T. (1985). *Sci. Sin.* B**28**, 835–843.

ZACHARIASEN, W. H. (1963). *Acta Cryst.* **16**, 1139–1144.

Acta Cryst. (1993). B**49**, 130–136

A Crystallographic and Molecular Mechanics Study of Inhibitors of Dihydroorotase

BY TREVOR W. HAMBLEY, LEONIDAS PHILLIPS, ANTHONY C. POINER AND RICHARD I. CHRISTOPHERSON

Departments of Inorganic Chemistry and Biochemistry, University of Sydney, NSW 2006, *Australia*

(*Received* 19 *May* 1992; *accepted* 20 *July* 1992)

Abstract

(I) Methyl L-dihydroorotate, $C_6H_8N_2O_4$, M_r = 172.14, orthorhombic, $P2_12_12_1$, a = 6.941 (2), b = 9.708 (2), c = 23.329 (5) Å, V = 1572 Å^3, Z = 8, D_x = 1.455 g cm^{-3}, Mo $K\alpha$, λ = 0.71069 Å, μ = 0.81 cm^{-1}, $F(000)$ = 720, T = 294 K, final R = 0.036 for 793 reflections. (II) Methyl L-6-thiodihydroorotate, $C_6H_8N_2O_3S$, M_r = 188.21, monoclinic, $P2_1$, a = 6.235 (2), b = 20.821 (4), c = 6.882 (1) Å, β = 110.82 (2)°, V = 835.0 Å^3, Z = 4, D_x = 1.497 g cm^{-3}, Mo $K\alpha$, λ = 0.71069 Å, μ = 3.02 cm^{-1}, $F(000)$ =

0108-7681/93/010130-07$06.00